The differential equation describing random walks on the Koch curve

2001 J. Phys. A: Math. Gen. 34 8397

(http://iopscience.iop.org/0305-4470/34/41/301)

INSTITUTE OF PHYSICS PUBLISHING JOURNAL OF PHYSICS A: MATHEMATICAL AND GENERAL

J. Phys. A: Math. Gen. **34** (2001) 8397–8406 PII: S0305-4470(01)27363-6

The differential equation describing random walks on the Koch curve

C Essex[1], M Davison[1], C Schulzky[1], A Franz[2] and K H Hoffmann[2]

[1] Department of Applied Mathematics, The University of Western Ontario, London, Canada N6A 5B7
[2] Institut für Physik, Technische Universität, D-09107 Chemnitz, Germany

Received 24 July 2001
Published 5 October 2001
Online at stacks.iop.org/JPhysA/34/8397

Abstract

Consider a particle which is released at some point on a fractal and which moves about the fractal at random. A long standing goal has been to determine a differential equation governing the probability density function which describes this walk. As well as being interesting in its own right, this problem is thought to provide an insight into the problem of anomalous diffusion. Many attempts to derive such an equation have been made, all with limited success, perhaps because of the tension between smoothness required by differential equation tools and the lack of smoothness inherent in fractals. Here we present, for the first time, the equation governing the random walk on a simple fractal—the Koch curve. We show that this equation makes computation of the probability density function for this problem a simple matter.

PACS numbers: 05.45.Df, 66.10.Cb, 05.40.Fb

1. Introduction

Random walks on fractal structures are frequently used to model anomalous diffusive behaviour in disordered media [1], e.g., to model the diffusion of hydrogen in amorphous metals [2] or of water in biological tissues [3], to mention only a few occurrences. All these processes are characterized microscopically by a time-dependent distribution of particles $P(r, t)$, where the mean square distance, $\langle r^2(t)\rangle$, a particle has moved in time t from its starting point is

$$\langle r^2(t)\rangle \propto t^{2/d_w} \tag{1}$$

where d_w is the random walk dimension of the underlying fractal structure.

In the literature, many suggestions [4–9] have been given to generalize the well known Euclidean diffusion equation

$$\frac{\partial}{\partial t}P(r,t) = \frac{\partial^2}{\partial r^2}P(r,t) \tag{2}$$

0305-4470/01/418397+10$30.00

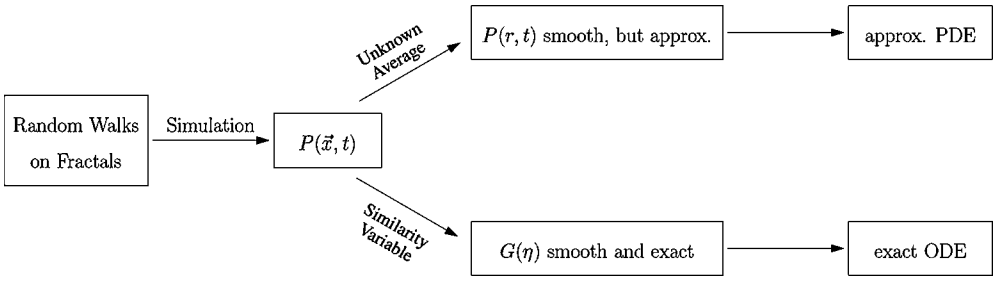

Figure 1. Difference of our approach to previous discussions of diffusion on fractals in the literature. Instead of averaging the data after the simulation, we impose the similarity transformation (3) and get a muscle-shaped cloud, such as the one depicted in figure 2. The fibres of this cloud are continuous functions of the similarity variable η and therefore predestinated for a description by an ordinary differential equation.

to anomalous diffusion. All these approaches, some including nonlinear equations [9] or even fractional derivatives [6–8], were at best partially successful [10] because a detailed and comprehensive physical theory for generalized diffusion equations, in terms of the underlying fractal dynamics, is still missing. Such a theory has proven to be much more difficult to construct than that for the Euclidean case since there is no simple Gauss law for a fractal. This law is needed to convert a simple balance equation into a differential equation.

The main reason for these complications is that fractals are, by definition, 'spiky' or 'rough'. As a result, walks on them are not naturally described by differential or integral equations, which require a certain degree of smoothness.

The common way to this obvious difficulty is to look at some type of averaged quantity (see figure 1, upper branch). But the type of angle averaging implied by $P(r,t)$ does not impart enough smoothness [4, 5, 10], so as a consequence, the probability density $P(r,t)$ is a fractal itself. We do not know the dynamics of the random walk on the fractal well enough to do the kind of physically meaningful averaging needed for smoothness. So far, averaging must still be considered as a hypothetical solution to this problem. However, the attempt to find a partial differential equation for diffusion on fractals using any kind of average has not succeeded.

A more promising starting point for describing random walks on fractals is the use of the natural similarity group of such a walk (see figure 1, lower branch). We use the observation that the probability density $P(r,t)$—and also all the cited generalized diffusion equations [10]—is invariant under a one-parameter group [11] and can be written in the form

$$P(r,t) = t^{-(d_\mathrm{f}/d_\mathrm{w})} G(\eta) \tag{3}$$

where d_f is the fractal dimension and $\eta = rt^{-1/d_\mathrm{w}}$ is the similarity variable.

In an earlier paper [12] we applied this approach to the Sierpinski gasket and plotted $G(\eta)$ rather than $P(r,t)$, reducing a 3D plot to a 2D plot. This was done by determining the probability density $P(r,t)$ for several distinct times t. These distributions turn out to be multivalued and even self-similar. They all can be plotted against the similarity variable η in one graph by applying equation (3). In figure 2, taken from [12], the resulting $G(\eta)$ is still multivalued and appears like a muscle-shaped cloud with intrinsic fibres, revealing an interesting structure of the random walk behaviour. All the information about the random walk is given by these fibres. Therefore it is possible to reconstruct the original density $P(r,t)$ using just the information from these fibres.

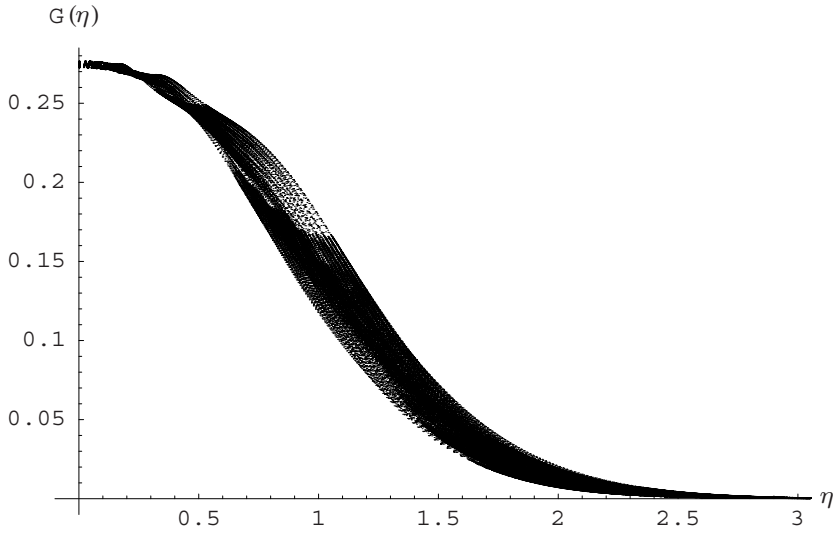

Figure 2. The muscle-shaped cloud $G(\eta)$ for the diffusion on a Sierpinski gasket. It is generated by taking the data $P(r, t)$ for many different times t and transforming them using equation (3). Note the fibres within the cloud, which can be shown to be continuous functions of η. This figure is taken from [12].

Finding an ordinary differential equation for these fibres, which turn out to be continuous functions of η, would completely describe the diffusion process on the considered fractal. This approach is much more promising than trying to construct a PDE for a somehow-averaged or even fractal probability density $P(r, t)$.

In this paper we apply the similarity solution method to the much easier case of the Koch curve taking the step from observation to understanding. For this prototype case we reproduce the fibres of the cloud by considering the well known diffusion on a line. The idea of echo point classes, proposed in [12], is also revisited and we present an ordinary differential equation for the smooth fibres allowing us to reproduce the fractal-like $P(r, t)$ gathered from simulations.

2. Random walk on the Koch curve

The Koch curve is constructed by dividing a line of length 2 units into three equal segments and replacing the middle part with two sides of an equilateral triangle of the same length as the removed segment. In the second iteration stage this procedure is repeated with each of the four segments of length $2/3$ units. The limiting case, after iterating this process an infinite number of times, is known as the Koch curve [13].

We consider a finitely generated Koch curve, such as the one depicted in figure 3, and set the coordinate origin at the apex of the centre triangle. Topologically, the M-times-iterated Koch curve is just a one-dimensional lattice. The *chemical distance* l of an arbitrary point x from the origin of the Koch curve is defined as the number of sites this point is away from the origin times Δx, where Δx is the Euclidean distance between two neighbouring points with $\Delta x = 2/3^M$ [14].

If we consider random walks on the Koch curve, starting at the origin, in terms of the chemical distance l, we can apply the well known results for diffusion on the line. For small

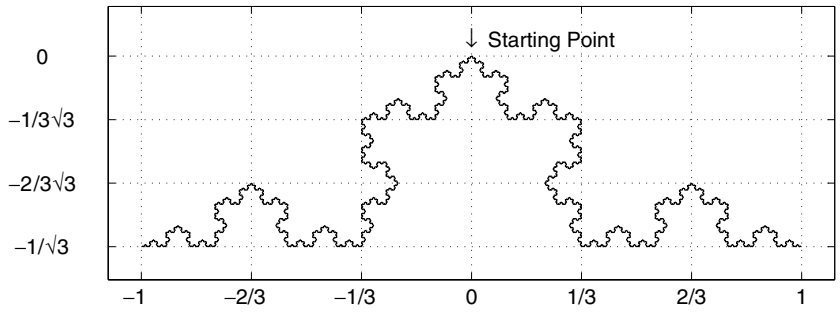

Figure 3. The six-time-generated Koch curve.

Δx and long times the resulting binomial distribution converges to a normal distribution, and thus the probability density function for the walk is

$$P(l,t) = \frac{1}{2\sqrt{D\pi t}} \exp\left(-\frac{l^2}{4Dt}\right) \tag{4}$$

where D is the diffusion constant. This smooth distribution tells us the probability of finding a particle at a point on the Koch curve which is at a certain chemical distance from the origin. Instead, we want to know the probability in terms of the Euclidean distance r at which this point is from the origin. Therefore we need the relation $l(r)$ for all points of the Koch curve.

To achieve this we recall some scaling exponents that characterize fractals. In the easy case of the Koch curve, the number of segments of the fractal, which is often referred to as the mass m of the fractal [14], scales in the same way as the chemical distance. Thus the chemical dimension d_l, defined as $m \sim l^{d_l}$ [14], equals 1. On the other hand, we immediately get the fractal dimension d_f from the construction process. This dimension is defined as the scaling exponent of $m \sim r^{d_\mathrm{f}}$. As the mass increases by a factor of 4, if we triple r we find $d_\mathrm{f} = \ln 4/\ln 3$ for the Koch curve.

The relation between the chemical distance l, which is the minimal length of a path between two points, and the Euclidean distance r is given by $l \sim r^{d_\mathrm{min}}$ with the scaling exponent d_min [14]. A comparison with the other mentioned scaling properties yields $d_\mathrm{min} = d_\mathrm{f}/d_l = d_\mathrm{f}$ and therefore:

$$l = \alpha\, r^{d_\mathrm{f}} \tag{5}$$

with the constant α.

Figure 4 shows a plot of the chemical distance versus the radial distance for each point of the Koch curve depicted in figure 3. Obviously the data show the predicted behaviour (5) on the average, but it also reveals the fractal nature of the Koch curve in the deviation from this power law.

Let us examine this in more detail by plotting the value of α versus r, where α is obtained as $\alpha = l/r^{d_\mathrm{f}}$ from the points of an M-generation Koch curve. To compare the values of α for different iteration stages M, the chemical distance must be rescaled. We rescale l such that in each iteration depth, the chemical distance from the origin to one of the two endpoints of the Koch curve in figure 3 has the value $l = 1$. Due to this rescaling, each point of the Koch curve keeps its chemical distance in higher iteration depths, i.e., when new intermediate points are introduced. Figure 5 shows this data for $M = 5$ (circles) and $M = 6$ (dots). As expected α for corresponding points in the different iteration depths are equal, a consequence of the self-similarity of the fractal. Another result is that the values for α are bounded and we find

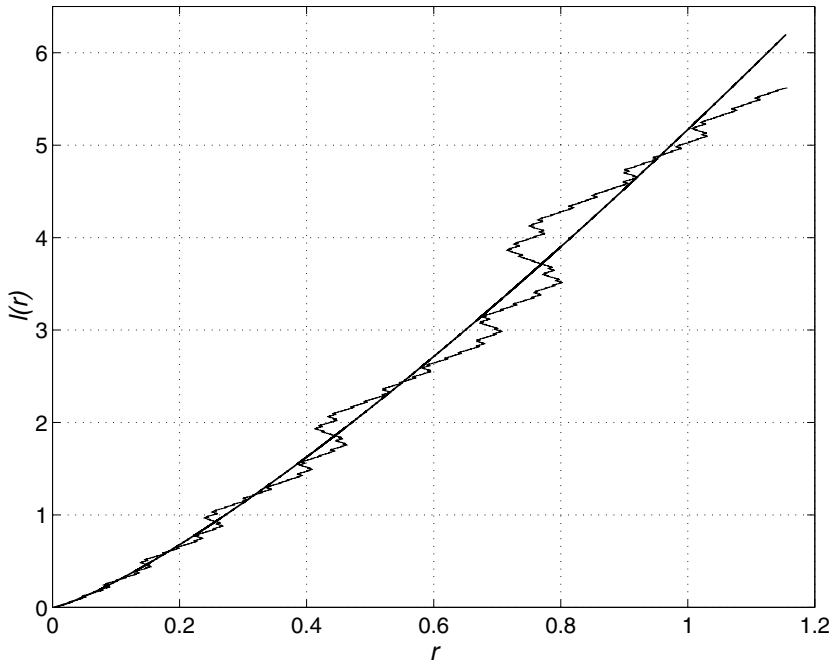

Figure 4. The relation between the chemical and Euclidean distances calculated for the Koch curve in figure 3. Note that the datapoints reflect the fractal essence of the Koch curve. The continuous curve represents equation (5), which yields the average behaviour.

$\alpha_{\min} = 0.823$ and $\alpha_{\max} = 1.07$. Because of the described scaling property, the extreme values of α converge for increasing iteration depths.

3. Echo point classes

The self-similarity of the Koch curve implies that the points that correspond to one another in different iteration stages have the same value of α. Let us examine the right neighbour of the starting point in a fixed iteration stage of the Koch curve, i.e., the solid circle denoted by x_1 in figure 6. As we do not compare the different iteration stages here, we do not have to rescale the chemical distance. Therefore this point has the Euclidean distance and also the chemical distance $r_1 = l_1 = \Delta x$ from the starting point with $\Delta x = 2/3^M$. Thus we get $\alpha_1 = l_1/r_1^{d_f} = (\Delta x)^{1-d_f}$. This point also defines a ray starting at the origin. For the next filled circle, x_2, on this ray one obtains $r_2 = 3\Delta x$ and $l_2 = 4\Delta x$ and thus $\alpha_2 = 4/3^{d_f}\alpha_1 = \alpha_1$, recalling that $d_f = \ln 4/\ln 3$. For all successive filled circles, $x_3, x_4, \ldots$, on this ray the Euclidean and chemical distances are multiplied each time by the factors 3 and 4, respectively. All these points have the same value $\alpha = \alpha_1$ and are therefore denoted as belonging to the same class of *echo points*.

Due to the symmetry of the rays, the points $y_1, y_2, \ldots$ also belong to the same echo point class. In figure 6 the line of symmetry is denoted by a dashed line. Note that the point y_1 has twice the chemical distance of x_1 and x_2 twice that of y_1 and so on. Summarizing this fact we can say that for every odd n, all points with chemical distance $l = 2^i n\Delta x, i = 0, 1, 2, \ldots$, belong to the same echo point class and have the same value of α (see figure 6).

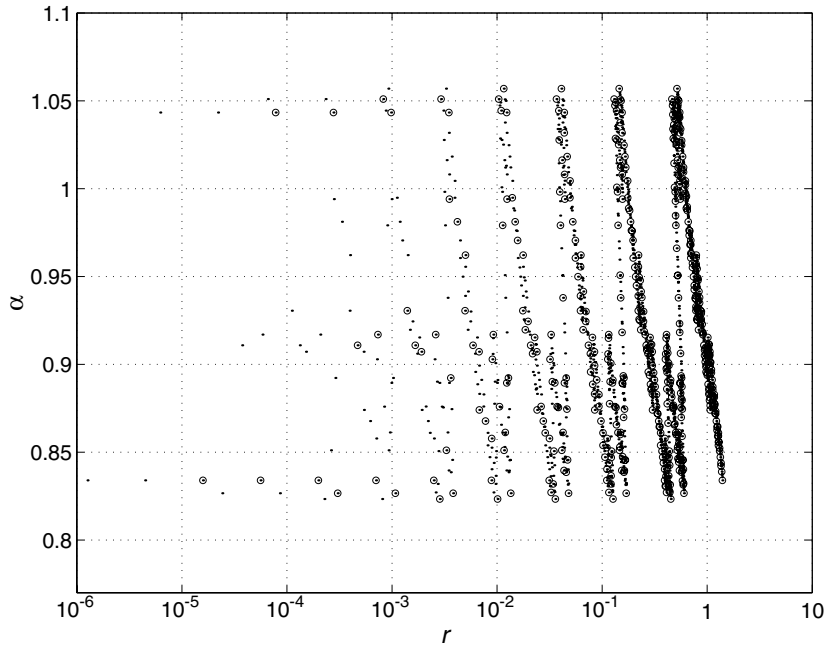

Figure 5. The deviation of the computed data for $l(r)$ to the predicted behaviour (5) by plotting $\alpha = l/r^{d_f}$ versus r. Note that the values for $M = 5$ (circles) fall exactly on the corresponding values from $M = 6$ (dots). Note also that the values of α are bounded.

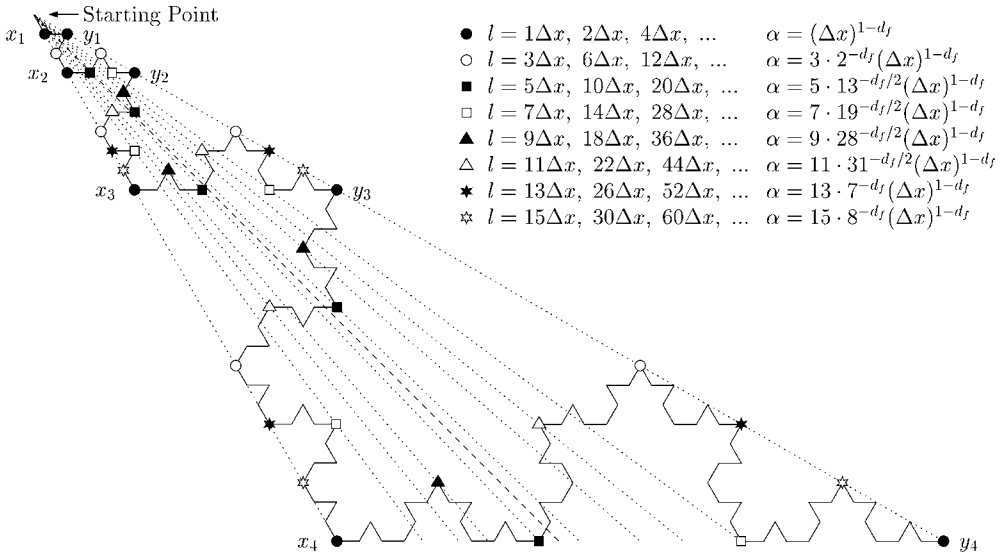

Figure 6. Echo point classes of the Koch curve. All points denoted by the same symbol have the same value for α. Note that the rays are symmetric with respect to the dashed line.

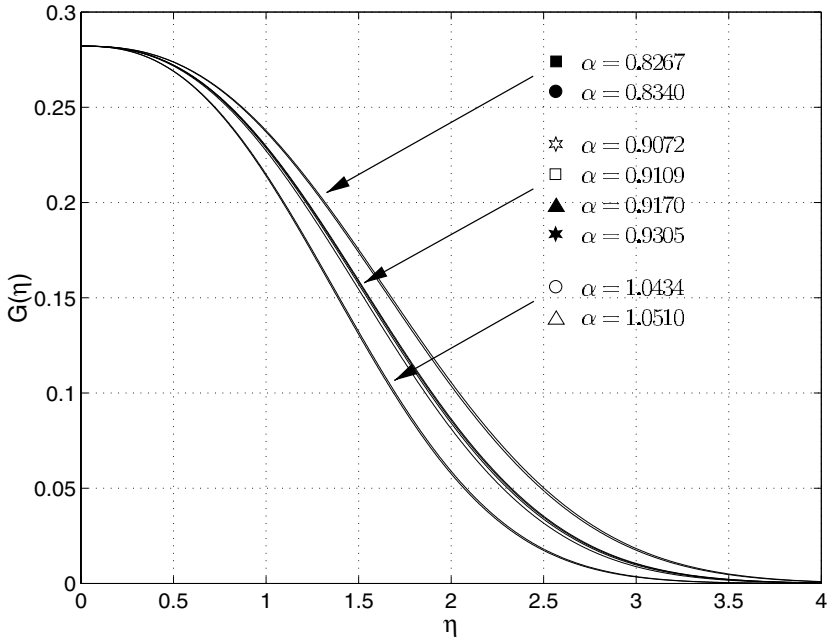

Figure 7. The fibres $G_\alpha(\eta)$ for all the echo point classes in figure 6 form a muscle-shaped cloud $G(\eta)$. Introducing more and more fibres will make the cloud denser. For this figure we used $D = 1$ in equation (7).

4. *G*-density on the Koch curve

Since we know the relation between l and r, we can now express the probability density $P(r, t)$ in terms of its scaling properties (3). As $P(r, t)$ is a fractal curve so is $G(\eta)$. We start by considering the point x_1 in figure 6. This point has a certain chemical distance l_1 and an Euclidean distance r_1 from the origin, and belongs to the echo point class with $\alpha_1 = (\Delta x)^{1-d_f}$.

As r and l are fixed for each point of the fractal, the time development of the probability of finding a walker at this point is given by equation (4) in terms of the chemical distance. The variable substitution $\eta = rt^{-1/d_w}$ changes the running variable from t to the similarity variable η and we find

$$P(l, t) = t^{-1/2} G_\alpha(\eta) \tag{6}$$

with

$$G_\alpha(\eta) = \frac{1}{2\sqrt{D\pi}} \exp\left(-\frac{1}{4D}\frac{l^2}{r^{d_w}}\eta^{d_w}\right) = \frac{1}{2\sqrt{D\pi}} \exp\left(-\frac{\alpha^2}{4D}\eta^{d_w}\right) \tag{7}$$

where we applied relation (5) and $d_w = 2d_f$, which is a special property of the Koch curve. As equation (7) just depends on α, and no longer on the distinct values of r or l, each member of an echo point class produces the same fibre $G_\alpha(\eta)$. These functions are stretched exponentials with the parameter α. As α has an upper and a lower boundary, a plot of $G_\alpha(\eta)$ for different echo point classes α looks like a muscle, where the top and bottom fibres are given by $\alpha_{\min}$ and $\alpha_{\max}$, respectively.

In figure 7 the values for the chemical distance and therefore also for α have been rescaled corresponding to the procedure described in section 2. The fibres for the first eight echo point classes (denoted by the symbols in figure 6) are plotted. Introducing more values of α makes

the cloud denser and the extremal values are represented more exactly. Nevertheless figure 7 gives a reasonable impression of the thickness of the cloud.

This muscle-shaped cloud $G(\eta)$ is very similar to the one found on the Sierpinski gasket [12] (compare figure 2), with two major differences: first, we do not encounter any wiggles here. We conjecture that these wiggles are a consequence of the lacunarity of the gasket. For a nonlacunar fractal, such as the Koch curve, the topological equivalence to a straight line implies the use of (4) which has no wiggles. Second, in the easy case of the Koch curve we are able to write down a closed form for $G_\alpha(\eta)$, which is an open question for random walks on other fractals.

5. ODE for diffusion on the Koch curve

Since we have a closed form for the smooth fibres (7) of the cloud, it is straightforward to find a differential equation for them. This describes the diffusive behaviour on the Koch curve.

An obvious choice is to seek a first-order differential equation as its solutions have one arbitrary integration constant, which in our case can be identified with the parameter α. From this viewpoint $G(\eta)$ represents a one-parameter family of functions, one for each α. To find the equation that yields this family of functions we calculate the logarithmic derivative of $G(\eta)$,

$$\frac{G'(\eta)}{G(\eta)} = \frac{\mathrm{d}}{\mathrm{d}\eta}\ln(G(\eta)) = -d_\mathrm{w}\frac{\alpha^2}{4D}\eta^{d_\mathrm{w}-1} = \frac{d_\mathrm{w}}{\eta}\ln\left(2\sqrt{D\pi}\,G(\eta)\right) \tag{8}$$

in order to eliminate the free parameter α. It follows that the ordinary differential equation

$$\eta\,G'(\eta) - d_\mathrm{w}\,G(\eta)\ln\left(2\sqrt{D\pi}\,G(\eta)\right) = 0 \tag{9}$$

has the desired family of solutions (7). It is clear from (8) that no other first-order ordinary differential equation will have this particular family of solutions.

6. Comparison with random walk data

To demonstrate the applicability of our results, we use equation (9) to find the probability density $P(r, t_0)$ of walkers on the Koch curve after a certain time $t = t_0$ with a start distribution $P(r, 0) = \delta(0)$ of the walkers.

The solution of the ordinary differential equation (9) is given by $G_\alpha(\eta)$ (see equation (7)), where α denotes the arbitrary constant, which can be chosen as $\alpha = l/r^{d_\mathrm{f}}$.

In this example we consider the first eight echo point classes (compare figure 6) and get the chemical and Euclidean distances for the first point of each of these classes directly by constructing a Koch curve of small iteration depth ($M = 3$ in the current case). The successive echo points in each class are then easily calculated by multiplying l and r by 2 and $\sqrt{3}$, respectively. In this manner all the echo points of all the considered classes for a given, but arbitrary, iteration depth are obtained.

Now we apply equations (6) and (7) to find the values of the probability density at all the considered points. Connecting the resulting points in an r–P plot should give a good approximation of the (multivalued) probability distribution $P(r, t)$ of random walkers on a Koch curve.

To check the quality of our approximation we simulate such a random walk by iterating the master equation in the chemical space,

$$P(l, t + \Delta t) = P(l, t) + w(P(l - \Delta l, t) + P(l + \Delta l, t)) - 2wP(l, t) \tag{10}$$

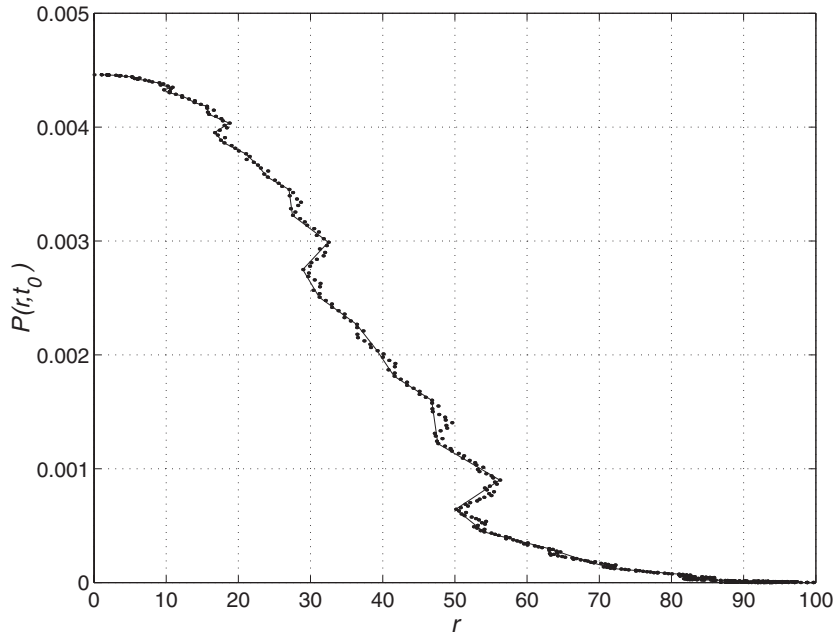

Figure 8. The probability density $P(r, t_0 = 10\,000)$. The data points (dots) are determined by applying the master equation (10) on a six-time-generated Koch curve with the transition probability $w = 0.4$. The solid curve is produced by using the information given by the fibres (7) for the first eight echo point classes described in figure 6.

where w is the transition probability from one site to another. If we choose $P(l = 0, t = 0) = 1$ and $P(l, 0) = 0$ for all other l, equation (10) becomes the discrete version of equation (4) with the diffusion constant $D = w(\Delta l)^2/\Delta t$ and a δ-function as start distribution.

Therefore we can compare the distribution that we get from the master equation at time $t = t_0$ with the approximation using the fibres, where we set the diffusion constant $D = w(\Delta l)^2/\Delta t$ in equation (7). Figure 8 shows such a comparison for $\Delta t = \Delta l = 1$ and $t_0 = 10\,000$ on a six-time-generated Koch curve. We have chosen $w = 0.4$ and thus we used $D = 0.4$ in equation (7). The approximation shows the basic features of the simulated distribution very well especially for small r. But even for larger r our approximation describes the basic behaviour of the probability distribution. To get a better result, we simply have to consider more echo point classes.

To stress the success of our approximation, we summarize this example. We calculate the chemical and Euclidean distances for just eight points using an iteration depth $M = 3$ of the Koch curve. Evaluating the fibres at these points and using the similarity approach (6), we get a very good approximation for the probability distribution on a six-time-generated Koch curve. The validity of this approach is not limited to this low iteration depth. It also works for very high iteration depths, where a numerical comparison with the master equation is not feasible anymore.

7. Conclusion

In this paper we address the problem of a random walker moving on a Koch curve. Instead of averaging the simulated data to obtain a somehow-smoothed probability density, we apply a

similarity group approach and deal with the multivalued G-density. The occurring fibres are calculated explicitly using the topological equivalence to a straight line.

For the first time an ordinary differential equation is given describing all the details of the diffusion process on a Koch curve. As a first application the probability density, commonly used for the discussion of the diffusion process, is arbitrarily well approximated. Thus the long standing goal to determine an equation governing the probability density function on a fractal is reached for the simple case of the Koch curve.

The described results can be easily generalized to any fractal that is topologically equivalent to a straight line. The generalization to more complicated, especially lacunar, fractals is also possible, at least in principle. The concept of fibres, clouds and echo points has already been described in [12] for the Sierpinski gasket. But an analytical function describing the fibres in this case has not been found yet and therefore no ordinary differential equation for them has been established. This is the topic of future work.

References

[1] Havlin S and Ben-Avraham D 1987 Diffusion in disordered media *Adv. Phys.* **36** 695
[2] Schirmacher W, Perm M, Suck J-B and Heidemann A 1990 Anomalous diffusion of hydrogen in amorphous metals *Europhys. Lett.* **13** 523
[3] Köpf M, Corinth C, Haferkamp O and Nonnenmacher T F 1996 Anomalous diffusion of water in biological tissues *Biophys. J.* **70** 2950
[4] O'Shaughnessy B and Procaccia I 1985 Analytical solutions for diffusion on fractal objects *Phys. Rev. Lett.* **54** 455
[5] O'Shaughnessy B and Procaccia I 1985 Diffusion on fractals *Phys. Rev.* A **32** 3073
[6] Giona M and Roman H E 1992 Fractional diffusion equation for transport phenomena in random media *Physica* A **185** 87
[7] Giona M and Roman H E 1992 Fractional diffusion equation on fractals: One-dimensional case and as symptotic behaviour *J. Phys. A: Math. Gen.* **25** 2093
[8] Metzler R, Glöckle W G and Nonnenmacher T F 1994 Fractional model equation for anomalous diffusion *Physica* A **211** 13
[9] Compte A and Jou D 1996 Non-equilibrium thermodynamics and anomalous diffusion *J. Phys. A: Math. Gen.* **29** 4321
[10] Schulzky C, Essex C, Davison M, Franz A and Hoffmann K H 2000 The similarity group and anomalous diffusion equations *J. Phys. A: Math. Gen.* **33** 5501
[11] Hoffmann K H, Essex C and Schulzky C 1998 Fractional diffusion and entropy production *J. Non-Equilib. Thermodyn.* **23** 166
[12] Davison M, Essex C, Schulzky C, Franz A and Hoffmann K H 2001 Clouds, Fibres, and Echoes: A new approach to studying random walks on fractals *J. Phys. A: Math. Gen.* **34** L289
[13] von Koch H 1904 Sur une Courbe Continue sans Tangente, Obtenue par une Construction Geometrique Elementaire *Arkiv Matematik, Astronomi och Fysik* **1** 681
[14] Bunde A and Havlin S (ed) 1996 *Fractals and Disordered Systems* (Berlin: Springer)